An Evaluation of Thermochemical Property Models for CaO-MnO-SiO_2-Al_2O_3-MgO Slag

J. MULLER and J.D. STEENKAMP*

**Exxaro Resources, Pretoria, South Africa*

Dept. of Materials Science and Metallurgical Engineering, University of Pretoria, Pretoria, South Africa

Abstract: The modeling of thermochemical properties is important in studying the physical behavior of slag in the operation of pyrometallurgical smelters. To study the flow of slag through a submerged-arc furnace (SAF) taphole, knowledge of thermochemical properties such as viscosity, thermal conductivity, density and heat capacity are required. In literature various models exist for silicate slags that enable thermochemical properties to be predicted as functions of chemical composition and temperature. This paper reports on the application of models in the CaO-MnO-SiO_2-Al_2O_3-MgO slag system to be used in future CFD modeling of slag tapped from SAFs producing high-carbon ferromanganese (HCFeMn) or silicomanganese (SiMn). FactSage 6.2 is used to estimate the phase composition of slags with varying chemical composition and temperature. The dependence of thermochemical property models on chemical composition and temperature is illustrated in the form of ternary diagrams showing the predicted property values as a function of basicity (chemical composition) and temperature. Slag compositions typical of HCFeMn and SiMn processes are used. Each thermochemical property is calculated at 1400, 1500 and 1600°C at a fixed weight percentage ratio Al_2O_3/SiO_2 of 0.57 and 6% MgO. Ternary phase diagrams (1400, 1500 and 1600°C) and a ternary liquidus temperature diagram are also presented for the system. Since viscosity has the most significant influence on flow behavior, results from various viscosity models have been compared with measured data. Predictions for thermal conductivity, density, and heat capacity are also discussed.

Key words: slag, density, heat capacity, thermal conductivity, viscosity, CFD

1. Introduction

Manganese ferroalloys can be classified into ferromanganese (FeMn) with varying carbon contents (high-, medium-, and low-carbon), and silicomanganese (SiMn) [1]. In South Africa both high-carbon ferromanganese (HCFeMn) and SiMn are produced from smelting manganese oxide ores and reductants in submerged-arc furnaces (SAFs). HCFeMn slags contain typically 15 to 20% MnO (discard slag practice), and SiMn slags approximately 9%. In both cases slag is discarded onto slag dumps. In other countries HCFeMn slags contains typically 30 to 50% MnO (high-MnO slag practice), and are fed to SAFs with ores, reductants, quartz and other fluxes to produce SiMn [2]. Typical slag compositions for the production of HCFeMn (high-MnO and discard slag practices) and SiMn are presented in Table 1.

The removal of slag from smelting furnaces is a key operational aspect in the production of HCFeMn or SiMn. Although both types of slag are manganese-bearing, differences in operating conditions and chemical compositions cause differences in thermochemical properties, leading to unfavorable behavior such as difficulties during slag taphole opening and sluggish or intermittent slag flow during tapping. Operators compensate for these adverse effects by

increasing the operating temperature, changing the slag chemistry, or lancing open tapholes. These actions may result in refractory damage over time, amongst other effects on the process and equipment. It is therefore important to study the CaO-MnO-SiO_2-Al_2O_3-MgO slag system to understand the underlying differences in the production of HCFeMn and SiMn specifically related to the influences of slag composition.

Table 1 Typical HCFeMn and SiMn slags used as baselines in the evaluation of thermochemical properties, partly sourced from literature [2].

Name	Reference	Normalized composition (mass%)					
		MnO	SiO2	Al2O3	CaO	MgO	Basicity*
HCFeMn Slag A	High MnO slag [2]	40.9	23.1	12.7	16.9	6.4	1.79
HCFeMn Slag B	Discard slag [2]	15.1	24	20.7	34.4	5.7	1.23
HCFeMn Slag C		29.8	30	4.3	29.3	6.6	1.91
HCFeMn Slag D		36	24	16	20	4	1.5
SiMn Slag A	Typical SiMn slag [2]	8.5	45.2	15.8	21	9.5	0.64
SiMn Slag B		7.7	42.1	20.9	22.4	6.9	0.59
SiMn Slag C		3.1	41.8	20	29	6.2	0.62

* Basicity = $(CaO+MgO+MnO)/(Al_2O_3+SiO_2)$

Typical process temperatures in SiMn production range from 1600 to 1650°C with the slag leaving the furnace between 1550 and 1650°C, while process temperatures in HCFeMn production range between 1400 and 1500°C [2].

This paper presents the first part of a study where the flow of manganese-bearing slag through electric furnace tap-holes is modeled using computational fluid dynamics (CFD) methods. Here the relevant thermochemical properties are evaluated and models presented, specifically for manganese-bearing slags, which are currently believed to provide the best estimations as functions of temperature and chemical composition. These models were applied in order to make predictions regarding the differences in properties of HCFeMn and SiMn slags, and subsequent heat and mass transfer behavior differences. These differences may then be verified through the application of these property models and evaluation of CFD models based on typical taphole designs and operating conditions and practices to determine the validity of these models and the measurements on which they are based.

2. Methodology

2.1 Heat and mass transfer flow modeling

To model the flow of mass and energy, the conservation of energy and momentum equations are considered. The dependent variable may be replaced to model heat transfer or mass flow as follows [3], illustrating why thermal conductivity, heat capacity, density and viscosity are thermochemical properties of interest when modeling a taphole:

- *Heat transfer*: The heat transfer equation in the x-direction only is given by the following where T is the dependent variable temperature (K), k the thermal conductivity ($W.m^{-1}.K^{-1}$), C_p the heat capacity ($J.kg^{-1}.K^{-1}$), ρ the density ($kg.m^{-3}$), S_x a term allowing for an additional energy source ($W.m^{-3}$) (e.g. heat of reaction), and u the velocity in the x-direction ($m.s^{-1}$).

$$\frac{\partial(\rho CpT)}{\partial t} + \frac{\partial(\rho CpuT)}{\partial x} = \frac{\partial}{\partial x}\left(k\frac{\partial T}{\partial x}\right) + S_x \quad (1)$$

- *Fluid flow*: For an incompressible fluid flow (no transient term, accumulation), the transport equation in the

x-direction only is given by the following where ρ is the density (kg.m^{-3}), u the velocity in the x-direction (m.s^{-1}), p the pressure (Pa), μ the fluid viscosity (Pa.s), g the standard gravity constant (9.81 m.s^{-2}), and S_x a term allowing for additional momentum source in the x-direction (e.g. body forces effect per unit volume).

$$\frac{\partial}{\partial t}(\rho u) + \mathrm{div}(\rho u \bar{u}) = div(\mu \,\mathrm{grad}\, u) - \frac{\partial p}{\partial x} + \rho g + S_x \quad (2)$$

2.2 Slag structure

The slag thermochemical properties of interest are dependent on the slag structure, which is determined mostly by its chemical composition and temperature [4]. Slags and glasses consist of four O^{2-} anions connected to a Si^{4+} cation arranged in a three-dimensional tetrahedral array [4]. Each of the O^{2-} anions can be connected to two other O^{2-} anions around the Si^{4+} cation and to another Si^{4+} cation, named "bridging oxygens", causing the formation of silicate polymer chains or rings [4]. An O^{2-} anion connected to only one Si^{4+} cation is named "non-bridging oxygen", with an O^{-} at the end of the chain. Basic oxides in the slag system (CaO, MgO, MnO) break up the silicate chains forming non-bridging (O^{-}) and free (O^{2-}) oxygen anions, decreasing the degree of polymerization [4] and influencing thermochemical properties.

Thermochemical properties are often modeled as functions of the optical basicity so as to consider the effect of polymerization. The number of non-bridging oxygens to tetragonal-bonded oxygens (*NBO/T*) may be estimated from the molar fractions of chemical slag constituents [5].

The fraction of non-bridging oxygen (*NBO*):

$$NBO = 2\,[X_{CaO} + X_{MgO} + X_{MnO} - 2X_{Al2O3}] \quad (3)$$

The fraction of tetragonal-bonded oxygen (*T*):

$$T = X_{SiO2} + 2X_{Al2O3} \quad (4)$$

The degree of polymerization (*Q*) is estimated:

$$Q = 4 - NBO/T \quad (5)$$

2.3 Metallurgical system

To model the thermochemical properties, the metallurgical system has to be defined. It is mostly determined by composition and temperature ranges. The predominant constituents and most likely solid and liquid phases at typical operating conditions are determined, and used to configure computational thermochemistry software applied in the calculation of thermochemical properties.

For the production of SiMn or HCFeMn the important thermochemical properties are evaluated for the CaO-MnO-SiO_2-Al_2O_3-MgO slag system only, ignoring all minor components (P, S, K_2O, Na_2O, TiO_2, etc.). The compositions in Table 1 are considered, together with temperatures from ambient conditions up to the maximum of approximately 1650°C, enabling the prediction of solid properties in areas where solidification might occur.

Thermochemical calculation software, FactSage 6.2 [6], was used to make predictions on phase compositions at

different temperatures. The metallurgical system was configured from solution- and pure constituent-phases with selections from mostly the FToxid database. The most important selected phases are [6]: slag liquid; monoxide solid solution; melilite; mullite; spinel; SiO_2 pure solid; and di-calcium silicate. The phases were selected with prior knowledge of solid and liquid phases expected for the system derived from published phase diagrams [2,4].

3. Discussion

3.1 Metallurgical system

Ternary phase diagrams were generated using FactSage 6.2 [6] for the system with 6% MgO, and an Al_2O_3/SiO_2 ratio of 0.57 (according to $Si_3O_6.Al_2O_3$), calculated at 1400, 1500 and 1600°C. The monoxide and di-calcium silicate solid solution phase boundary lines indicate the liquidus points for HCFeMn and SiMn slags. From the results a ternary liquidus temperature diagram was generated reporting liquidus temperatures between 1200 and 2000°C (Figure 1), with HCFeMn and SiMn slags (Table 1) normalized to 6% MgO indicated. Solidus and liquidus temperatures calculated specifically for the SiMn and HCFeMn slags (Table 1) are provided in Table 2. These values vary slightly from those of the ternary liquidus diagram as a result of normalization to 6% MgO.

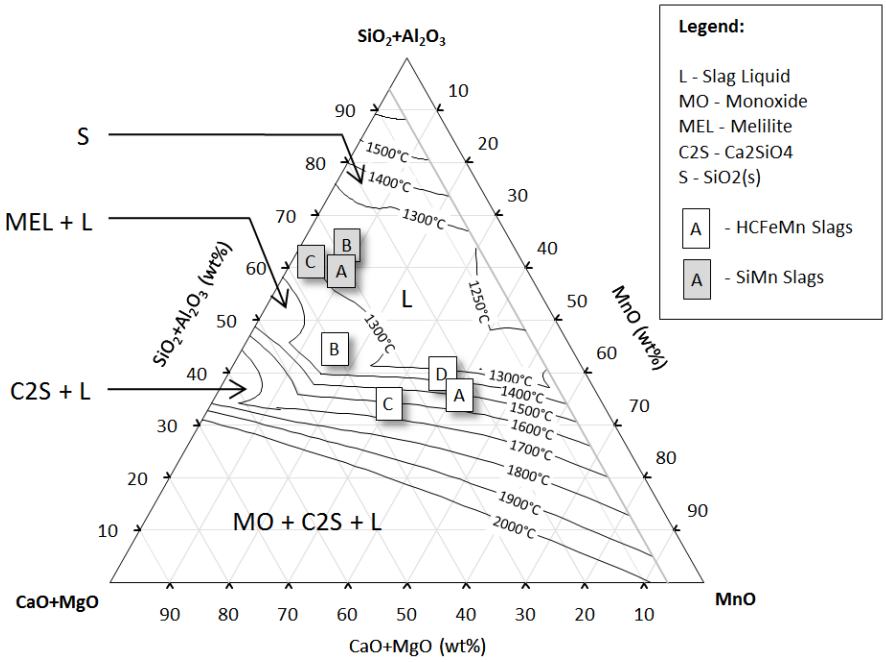

Fig. 1 Liquidus temperature diagram of the CaO-MnO-SiO_2-Al_2O_3-MgO slag system with 6% MgO and Al_2O_3/SiO_2= 0.57, showing SiMn and HCFeMn slag compositions (Table 1), calculated with FactSage 6.2 [6].

Table 2 Solidus and liquidus temperatures of SiMn and HCFeMn slag compositions (Table 1) calculated with FactSage 6.2 [6].

	Solidus temperature (°C)	Liquidus temperature (°C)
HCFeMn Slag A	1121.7	1501.2
HCFeMn Slag B	1166.9	1418.5
HCFeMn Slag C	1128.7	1443.7
HCFeMn Slag D	1106.1	1323.4
SiMn Slag A	1071.6	1232.9
SiMn Slag B	1074.7	1310.3
SiMn Slag C	1072.4	1295.7

HCFeMn slags have higher liquidus temperatures than SiMn slags, as a result of the higher monoxides concentration forming higher-melting solids in HCFeMn slags. At operating conditions both the SiMn slags are tapped well above their liquidus temperatures, while the HCFeMn slags are operated closely around their liquidus temperatures with their thermochemical properties expected to be sensitive to temperature. SiMn slags are located in a region of the ternary liquidus diagram (Figure 1) where variations in chemical composition have little effect on the liquidus temperature compared to HCFeMn slags, where liquidus temperatures are predicted to vary with amounts of SiO_2 and Al_2O_3.

3.2 Viscosity

Viscosity is the convective term constant of the momentum conservation equation (Eq. 2). In general it is indicative of resistance to flow and the ease with which slag of a certain composition flows at a specific temperature. This is relevant in specific areas including flow through a taphole. Single-phase metallurgical slags behave as Newtonian fluids with viscosity being the proportionality constant between the shear stress and strain rate (at lower strain rates), independent of the strain rate value [7]. Therefore slag viscosity is related only to composition and temperature, irrespective of the forces acting on it. Multiphase slags (with suspended solids) behave reportedly as Newtonian and non-Newtonian fluids, with Newtonian behavior when the solid content is less than 10 to 40 volume percent [7]. Viscosities of slags are measured experimentally, with experimental errors in the order of ±25%. Experimental methods include oscillating-, falling-body, rotating, and capillary methods [8, 9, 10].

3.2.1 Viscosity modeling

Slag viscosity is normally modeled with consideration of it being largely dependent on slag structure. Higher degrees of polymerization lead to higher viscosities owing to the increased resistance of longer chains moving over each other. The addition of basic components (CaO, MgO and MnO) breaks up silicate chains and therefore lowers viscosities, increasing the ease with which slag flows. Viscosity-temperature dependence is normally modeled by Arrhenius-type relationships [8], where the pre-exponential factors and activation energies are related to chemical component amounts in the available models through different types of empirical relationships.

Below the liquidus temperature, slags containing 40% or less precipitated solids may still be considered Newtonian fluids [7]. The liquid viscosity (μ_{liq}) estimated with the typical models mentioned above are adapted with a relationship such as the Roscoe equation [11] to predict the effective viscosity, μ_{eff}, using the volume fraction solids ($\emptyset$) (may be estimated using Gibbs free energy minimization in FactSage 6.2 [6]):

$$\mu_{eff} = \mu_{liq}(1 - 1.35\,\emptyset)^{-2.5} \quad (6)$$

A number of viscosity models optimized for certain systems can be found in the literature [4, 5, 8]. A common, and easy to use, model is the Urbain formalism, which has been developed for various types of slags [4, 5]. In this model viscosity is related to temperature with the Weymann viscosity-temperature relationship. The pre-exponential constant and activation energy are correlated to the sum of mole fraction of slag constituents grouped into glass formers (SiO_2), modifiers (CaO, MgO, MnO) and amphoterics (Al_2O_3), where the contribution of some other species might be weighted [5]. Other models considered for this study are models by Riboud and Iida [5], and by Tang et al. [12].

FactSage 6.2 is also used to model viscosities of liquid slags and glasses, based on the "Modified Quasichemical Model", with data from the thermodynamic databases providing quantified estimation of the slag structure [6].

3.2.2 Model validation

The viscosity models have been applied and validated against measured data reported by Kozakevitch (3 to 5 Poise), Sørlie (6.4 to 372.3 Poise), Benesch (3.7 to 4.3 Poise) [12], and Chubinidze (1.4 to 2 Poise), similarly to the method used in model development by Tang *et al.* [12]. Data used here is referenced in the paper by Tang *et al.* [12]. Correlation plots of estimated versus measured viscosities reported by the former two authors are illustrated in Figure 2, showing better correlations than those obtained with the data reported by the latter two authors. For the data reported by Kozakevich the model by Tang *et al.* [12] offered the best approximations, while for the data reported by Sørlie the Urbain model by Mills *et al.* [5] produced estimations closest to the measured values in the viscosity range of interest (less than 20 Poise).

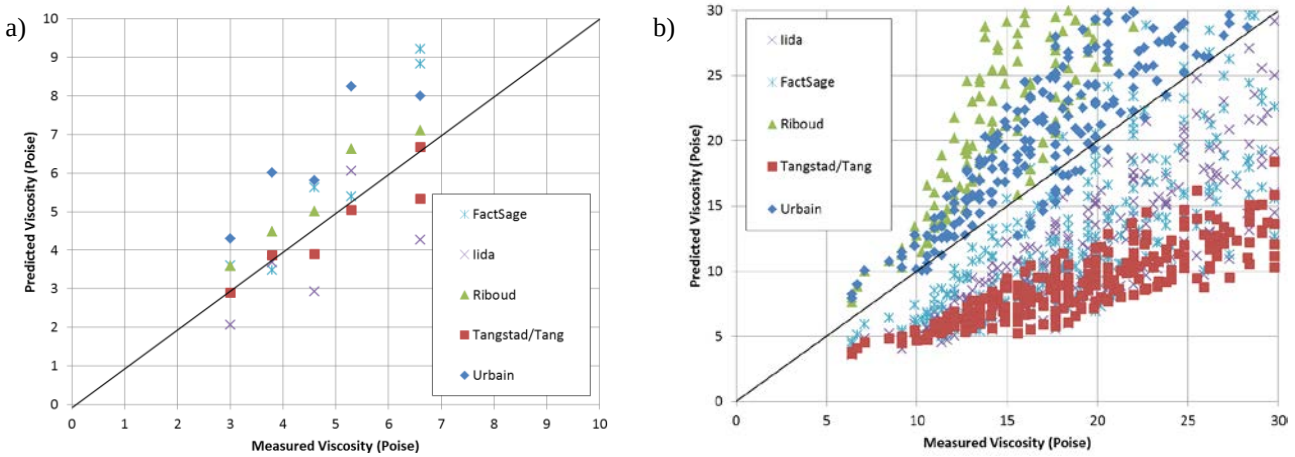

Fig. 2 Correlation plots of estimated viscosities vs. measured data by a) Kozakevitch, and b) Sørlie, as referenced by Tang *et al.* [12].

3.2.3 Sensitivity analysis

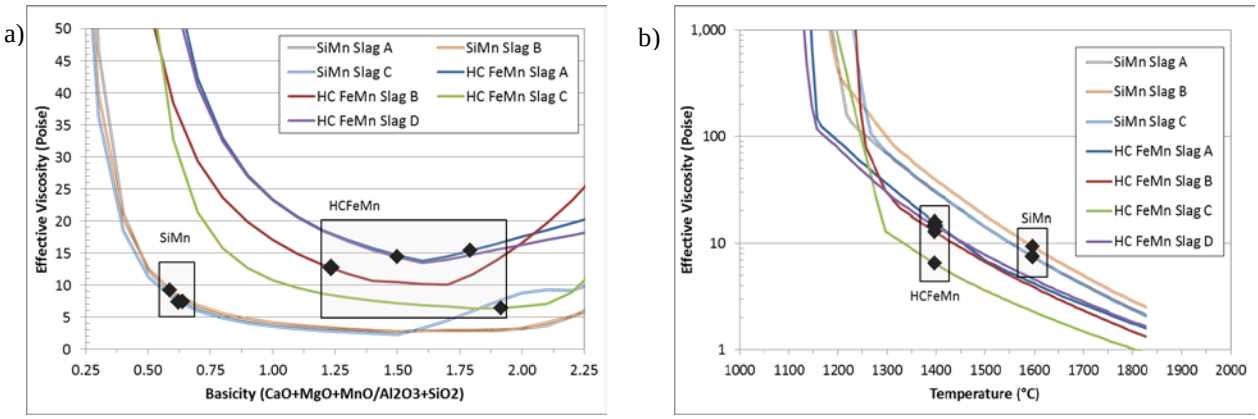

Fig. 3 Effective viscosity as a function of a) basicity ($CaO+MgO+MnO/SiO_2+Al_2O_3$) at operating temperatures of 1400°C for HCFeMn slags and 1600°C for SiMn slags, and b) temperature (°C), calculated using the Urbain model by Mills *et al.* [5], FactSage 6.2 [6], showing values for baseline compositions as points (Table 1).

Liquid viscosities at different temperatures (possibly multi-phase) have been estimated using the Urbain model reported by Mills *et al*. [5], the volume fraction solids using FactSage 6.2 [6], and the effect of the suspended solids incorporated using the Roscoe equation [11]. Using the SiMn and HCFeMn slag compositions (Table 1) as baselines, basicity (Figure 3a) and temperature (Figure 3b) have been varied to test sensitivity of the estimated effective viscosity to these parameters. For HCFeMn slags the baseline temperature of 1400°C was used, and for SiMn 1600°C.

3.2.4 Ternary diagram

Effective viscosities calculated for the SiO_2-CaO-MnO-Al_2O_3-MgO system at 1500°C with 6% MgO and Al_2O_3/SiO_2=0.57 are illustrated on the ternary diagram (Figure 4) as iso-effective viscosity lines. Diagrams were also generated for temperatures 1400°C and 1600°C, but are not included in this paper.

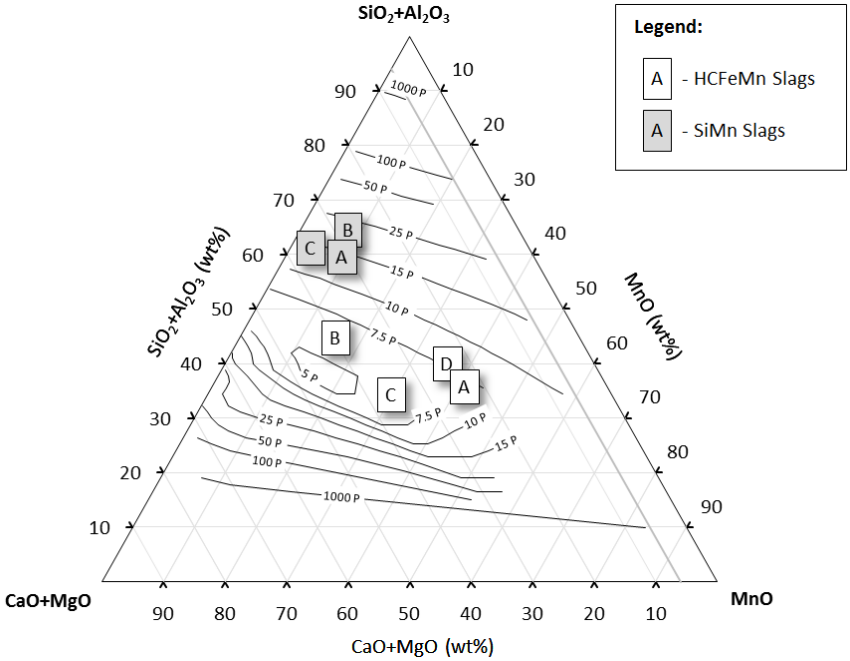

Fig. 4 Iso-effective viscosity ternary diagram (Poise) of the CaO-MnO-SiO_2-Al_2O_3-MgO slag system with 6% MgO and Al_2O_3/SiO_2= 0.57 at 1500°C, showing SiMn and HCFeMn slag compositions (Table 1). Calculated using the Urbain model by Mills *et al*. [5], FactSage 6.2 [6], and the Roscoe equation [11].

Characteristic of these diagrams is the decrease in viscosity moving up from the lower SiO_2 contents, due to the decreasing amounts of solids as the liquidus is approached (lowest viscosities). Above the liquidus (in the fully liquid region) the opposite is obtained, as viscosities then increase due to longer polymer chains forming. Iso-viscosity lines are therefore located (almost in parallel) around the liquidus compositions. Iso-viscosity lines are spread out further in the upper fully liquid slag phase region, compared to the lower multi-phase region. The slag viscosity is therefore predicted to be more sensitive to the effect of precipitation of solids than to the elongation effect of polymer chains.

SiMn slags are positioned in the single-phase regions where the viscosity is less sensitive to variations in SiO_2, compared to HCFeMn slags in the multi-phase regions with high sensitivity to variations in SiO_2. Viscosities of SiMn slags do not appear very sensitive to variations in MnO content (as reduction progresses), compared to HCFeMn slag

where the viscosity could likely decrease as reduction progresses with less MnO-based precipitated solids.

3.2.5 Conclusions

From the estimated effective viscosity results, the following are concluded:

- At 1600°C SiMn slags have no precipitated solids predicted and slightly lower viscosities, compared to HCFeMn slags at 1400°C having small amounts of solids and slightly higher viscosities.
- Increasing basicity would cause viscosities of SiMn slags to decrease due to networking-breaking monoxides, while viscosities tend to increase for HCFeMn slags as monoxide phase solids precipitate.
- Above the liquidus viscosity, increases in SiO_2 content form longer polymer chains which increase resistance to flow, while below the liquidus higher SiO_2 contents lead to the formation of less flow-hindering precipitated solids.
- SiMn slags with fixed $CaO+MgO/SiO_2+Al_2O_3$ ratios (a function of ore and fluxes) should have very consistent viscosity behavior, and are expected to be not as sensitive to the degree of reduction as might be the case with HCFeMn slags.

3.3 Thermal conductivity

Thermal conductivity is the diffusivity constant of the conductive term of the heat transfer equation (Eq. 1), representing ability of a specific material to conduct heat, given a temperature gradient and length. Thermal conductivity of metallurgical slags is important, especially when considering that the flow of energy affects the slag temperature, phase composition, and therefore other thermochemical properties. For example, in the taphole area during tapping the thermal conductivity would affect the temperature gradient throughout the tap stream, and then also the amount of precipitated solids and viscosity, influencing the fluid flow behavior and in turn the heat flow [13].

Thermal conductivities of slags can be experimentally determined through a number of techniques which mostly measure the heat flux. Steady-state or transient experimental methods include the laser-flash method [5, 14], the hot-wire method [14], the linear/radial heat flow method [4], and the phase-shift method [4]. Due to the nature of these experimental methods, measured results are very sensitive to the accuracy with which the experiments are executed [5, 14].

3.3.1 Thermal conductivity modeling

Thermal conductivity of slags is related to chemical composition and temperature, with distinctively different behavior and models dependent on whether the slag is liquid, glassy or crystalline [5]. Slag thermal conductivity is structurally dependent. It increases with increasing SiO_2 content due to the high thermal conductivity of covalently-bonded Si^{4+} and Al^{3+} ions [5]. The movement of phonons is easier along polymer chains than from end to end. Direct correlations exist between thermal conductivity and Q (Eq. 5), or inversely to the ratio of non-bridging oxygen to tetragonal-bonded oxygen (*NBO/T*). Correlations are derived between measured thermal conductivities and modeled slag viscosities.

Over the temperature range, thermal conductivity varies with dependence on the slag being glassy, crystalline or fully liquid. The thermal conductivity of crystalline slags is measured to be 1.5 to 2.5 times that of glassy or amorphous slags, and this is explained by the increased packing densities of crystalline slags. The apparent conductivity of glassy slags is,

however, larger than that of crystalline slags, in which radiation conductivity is decreased due to scattering [5]. The positive dependence of slag thermal conductivity on temperature is due to the increase in collision frequency and decrease of phonon mean free path [10], but packing density and changes in the silicate network have greater effects.

The models reported by Mills *et al*. [5] have been considered for this study. Thermal conductivities of solidified slag are estimated at 298K and at the glass transition temperature, both as functions of *Q* (Eq. 5). Thermal conductivities between these temperatures are obtained through linear interpolation. For liquid slags the model consisted of measured thermal conductivities correlated with modeled viscosities (using the Riboud viscosity model [5]). The glass transition temperature has been assumed 700°C, and the melting temperature the liquidus temperature (Table 2).

3.3.2 Sensitivity analysis

Slag thermal conductivities have been estimated using the models discussed above [5], predicting values as functions of basicity (Figure 5a) and temperature (Figure 5b) from the baseline compositions (Table 1).

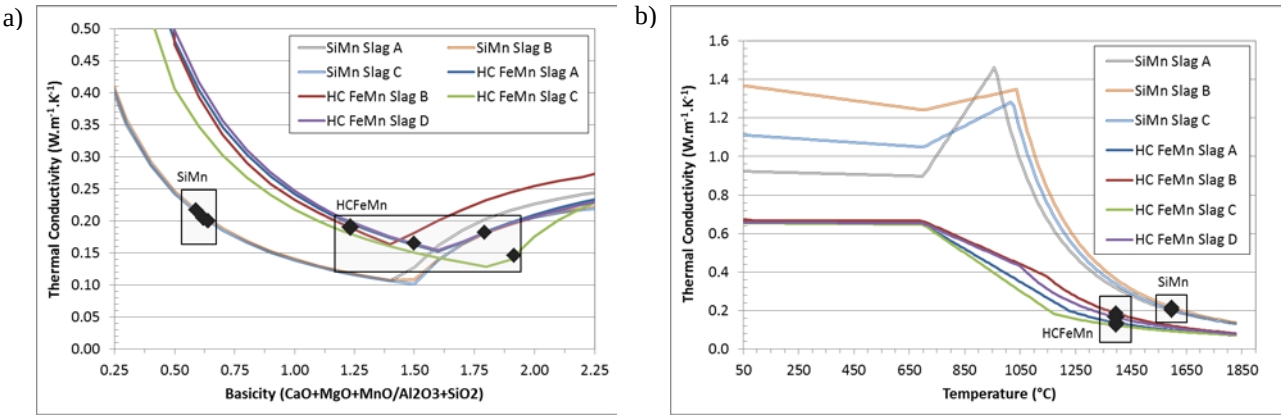

Fig. 5 Thermal conductivity as a function of a) basicity ($CaO+MgO+MnO/SiO_2+Al_2O_3$) at the operating temperatures of 1400°C for HCFeMn slags and 1600°C for SiMn slags, and b) temperature (°C), calculated using reported models [5] and FactSage 6.2 [6], showing values for baseline compositions as points (Table 1).

3.3.3 Ternary diagram

Thermal conductivities calculated for the SiO_2-CaO-MnO-Al_2O_3-MgO system at 1500°C with 6% MgO and Al_2O_3/SiO_2=0.57 are illustrated on the ternary diagram (Figure 6) as iso-thermal conductivity lines. Diagrams were also generated for temperatures 1400°C and 1600°C, but are not included in this paper. Estimated thermal conductivities are the lowest around liquidus composition, increasing towards both high and low SiO_2 contents, similar to Figure 5a. Thermal conductivities of both SiMn and HCFeMn slags are fairly insensitive to variance in the degree of MnO reduction.

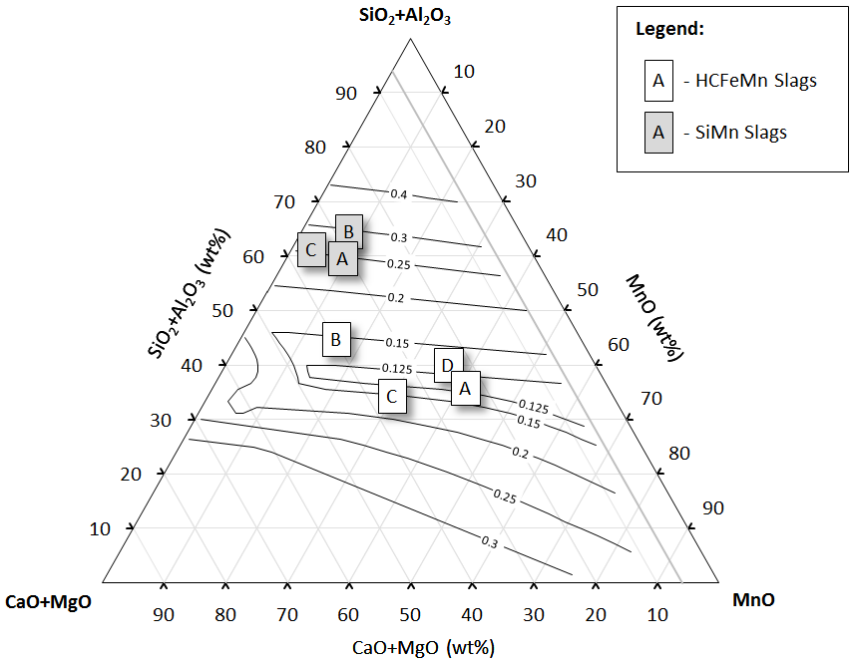

Fig. 6 Iso-thermal conductivity ternary diagram ($W.m^{-1}.K^{-1}$) of the CaO-MnO-SiO_2-Al_2O_3-MgO slag system with 6% MgO and Al_2O_3/SiO_2=0.57 at 1500°C, showing SiMn and HCFeMn slag compositions (Table 1). Calculated using the models by Mills [5].

3.3.4 Conclusions

From the estimated thermal conductivity results, the following conclusions can be drawn:

- At temperatures of 1600°C SiMn slags have slightly higher thermal conductivity than HCFeMn slags at 1400°C.
- At lower basicities thermal conductivity decreases with basicity due to the slags being liquid, and is directly proportional to viscosity, while at higher basicities it increases due the precipitation of conductive solids.
- From ambient temperature thermal conductivity increases slightly with temperature up to the liquidus temperature, after which it decreases sharply due the formation of less conductive liquid.
- Over the temperature range thermal conductivities of SiMn slags are significantly larger than that of HCFeMn slags, with higher SiO_2 contents leading to higher degrees of polymerization and longer, more conductive chains.

3.4 Density

Density simply refers to the mass of material per unit volume, featuring in the heat transfer equation (Eq. 1) with mass-specific heat capacity in both transient and convective terms, and present in several terms of the transport equation (Eq. 2). Density is measured using techniques and equipment that includes pycnometry, the Archimedes principle, a dilatometer, a manometer, droplet methods, and suspension methods [4].

3.4.1 Density modeling

Density of slags is estimated through summation of the partial molar volumes of the slag constituents, of which some are reported as functions of temperature [4]. Density is directly proportional to relative affinities between particles; it decreases with temperature as affinities become weaker [15] and relates to temperature with the thermal expansion

coefficient, α [4]. It has been reported that the thermal expansion coefficient increases with optical basicity, making slags with high optical basicities (lower degrees of polymerization) more sensitive to temperature [15]. Constituents such as SiO_2 are therefore associated with low thermal expansion, while density also increases with cation size [5].

To model density, molar volumes of slag constituents at specific temperatures and constant thermal expansion coefficients are taken from the literature [4]. For modeling the densities of solid slags the documented molar volumes for crystalline slag constituents at 25°C have been used [5]. A constant thermal expansion coefficient of 9 x $10^{-6}K^{-1}$ is used to calculate density up to the glass transition temperature [5]. The densities of glassy slags are calculated in a similar fashion up to the glass transition temperature, beyond which density is interpolated between solid density at the glass transition temperature and liquid density at the melting temperature [5]. Densities of liquid slags were estimated from published molar volumes at 1500°C [4] and constant positive thermal expansion of molar volume of 0.01 $\%.K^{-1}$ [5]. The glass transition temperature has been assumed to be 700°C, and the melting temperature the liquidus temperature (Table 2).

3.4.2 Sensitivity analysis

Slag densities have been estimated, predicting values as functions of basicity (Figure 7a) and temperature (Figure 7b) from the baseline compositions (Table 1).

a)

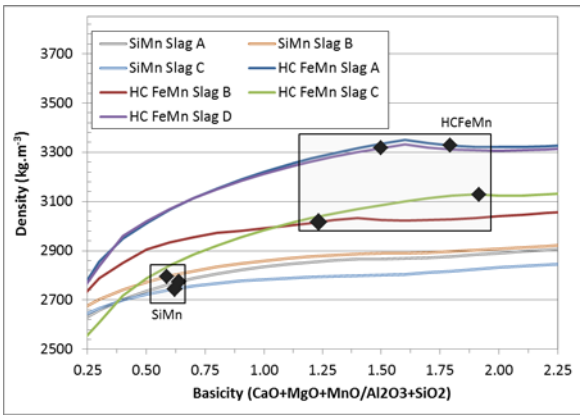

b)

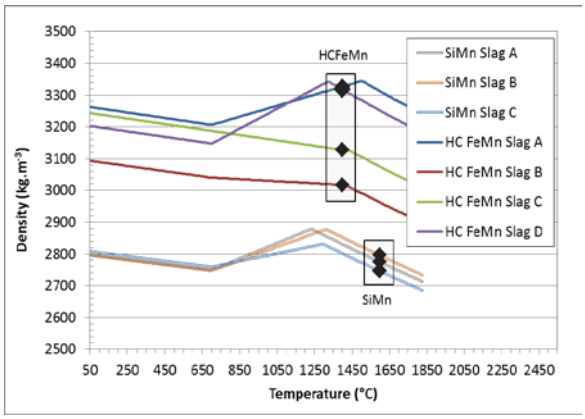

Fig. 7 Density as a function of a) basicity ($CaO+MgO+MnO/SiO_2+Al_2O_3$) at 1400°C for HCFeMn slags and 1600°C for SiMn slags, and b) temperature (°C), calculated using reported models [5] and FactSage 6.2 [6].

3.4.3 Ternary diagram

Densities calculated for the SiO_2-CaO-MnO-Al_2O_3-MgO system at 1500°C with 6% MgO and Al_2O_3/SiO_2=0.57 are illustrated on the ternary diagram (Figure 8) as iso-density lines. Diagrams were also generated for temperatures 1400°C and 1600°C, but are not included in this paper. At 1500°C the densities of HCFeMn slags are predicted somewhat higher than for SiMn slags. Density is predicted to be fairly insensitive to basicity ($SiO_2+Al_2O_3$/MgO+CaO), and depends largely to MnO content (with smaller partial molar volume), with density decreasing significantly as MnO reduction occurs.

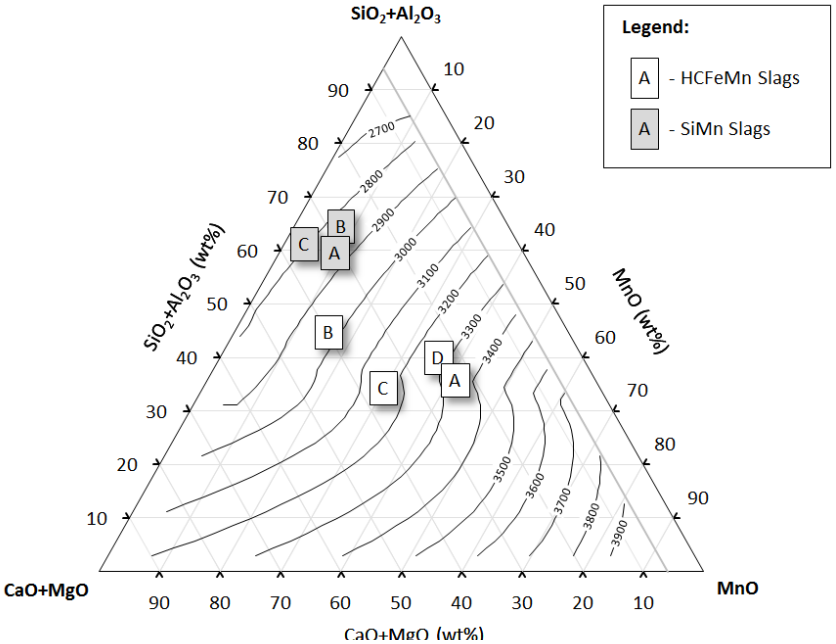

Fig. 8 Iso-density ternary diagram (kg.m^{-3}) of the CaO-MnO-SiO_2-Al_2O_3-MgO slag system with 6% MgO and Al_2O_3/SiO_2= 0.57 at 1500°C, showing SiMn and HCFeMn slag compositions (Table 1). Calculated using the models by Mills [5].

3.4.4 Conclusions

From the estimated density results, the following conclusions can be drawn:

- In the model MnO and other basic oxides have lower partial molar volumes compared to SiO_2 and Al_2O_3. The result is that density increases somewhat with basicity, and SiMn slags have significantly lower densities than HCFeMn slags.
- Over the basicity range the densities of SiMn slags are predicted to be significantly lower than for HCFeMn slags, due to the difference in baseline temperatures for which the results were calculated (1400°C for HCFeMn- and 1600°C for SiMn-slags) as well as SiMn slags having higher SiO_2 contents with high molar volumes.

3.5 Heat capacity/enthalpy

Heat a capacity is the relation between a change in material temperature and its heat content, and the derivative of enthalpy with regards to temperature. In the mass and energy flow applications of interest, heat capacity features in the transient and convective terms of the heat transfer equation (Eq. 1). Over time the fluid temperature response is dependent on the amount of mass and heat transferred in a time step and the heat capacity of the fluid. Other temperature-dependent properties (e.g. viscosity, thermal conductivity, density) are indirectly related to heat capacity. Heat capacities of slags are measured using commercially available differential scanning calorimeters (DSCs), or drop calorimeters.

3.5.1 Heat capacity modeling

Enthalpies (and heat capacities) of slags are functions of chemical composition, temperature, and structure [5]. Heat capacities and enthalpies can be estimated with models available in the literature. Due to limited dependence on

structure, heat capacity is typically modeled as partial molar properties, obtaining the net values by combining the values of the constituents over the temperature range, also modeling the energies required for phase change at specific temperatures (e.g. from crystalline solid to liquid slag). It is reported that the heat capacity of glassy slags is approximately 200 $J.kg^{-1}.K^{-1}$ higher than that of crystalline slags, so that the enthalpy does not undergo a step change at the melting temperature [5].

To model heat capacity (and enthalpy) the software FactSage 6.2 [6] has been used. Model parameters are stored in a database as temperature-dependent heat capacity equation coefficients and interaction parameters. Enthalpy results reflect heats of fusion, and phase transformation. The enthalpy model by Björkvall [16] has also been applied, based on a thermodynamic model developed for multicomponent slags by combining experimental data for binary sub-systems. The model predicts the enthalpy of multicomponent liquid slags by extrapolating for temperature from the enthalpies at 1600°C and using the heat capacity around that temperature for the pure species. Heat of fusion for the liquid phase is added, calculated from binary cation interactions.

Also applied were the heat capacity models reported by Mills [5], which estimate heat capacity of glassy, crystalline, and liquid slags considering it as a partial molar property, therefore combining the temperature-dependent heat capacities of each constituent. For crystalline slags, temperature-dependent equations are provided to predict the heat capacity of each component, while constant values are used for the liquid slag phase.

3.5.2 Sensitivity analysis

The enthalpies at certain temperatures relative to the reference state (298K) have been calculated using FactSage 6.2 software [6], testing the sensitivity to varying basicity (Figure 9a) and temperature (Figure 9b).

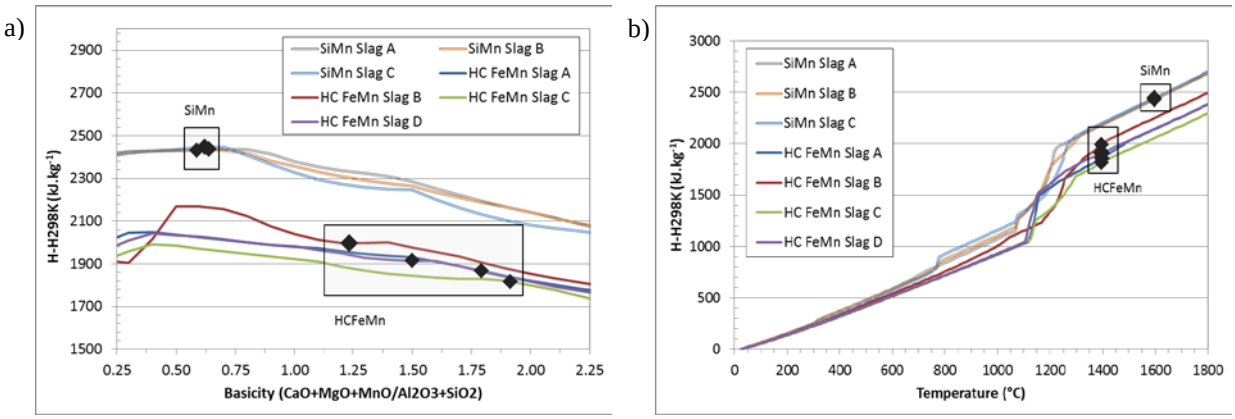

Fig. 9 H_T-H_{298K} as a function of a) basicity ($CaO+MgO+MnO/SiO_2+Al_2O_3$) at the operating temperatures of 1400°C for HCFeMn slags and 1600°C for SiMn slags, and b) temperature (°C), calculated using FactSage 6.2 [6].

3.5.3 Ternary diagram

Heat capacities calculated for the SiO_2-CaO-MnO-Al_2O_3-MgO system at 1500°C with 6% MgO and Al_2O_3/SiO_2=0.57 are illustrated on the ternary diagram (Figure 10) as iso-heat capacity lines. Diagrams were also generated for temperatures 1400°C and 1600°C, but are not included in this paper. The transition from solid to liquid is observed with increasing amounts of the SiO_2 and Al_2O_3 (between 30 to 50% $SiO_2+Al_2O_3$). Across this liquid

transformation line the increase in heat capacity is predicted to be approximately 200 to 300 $J.kg^{-1}.K^{-1}$. Below the liquidus compositions (lower amounts of SiO_2+Al_2O_3) heat capacities are predicted to increase mostly with amounts of SiO_2+Al_2O_3 and with decreasing amounts of MnO, having a range of approximately 200 $J.kg^{-1}.K^{-1}$. Above liquidus compositions heat capacity is predicted to vary with amounts of MnO, with a range of only approximately 100 $J.kg^{-1}.K^{-1}$

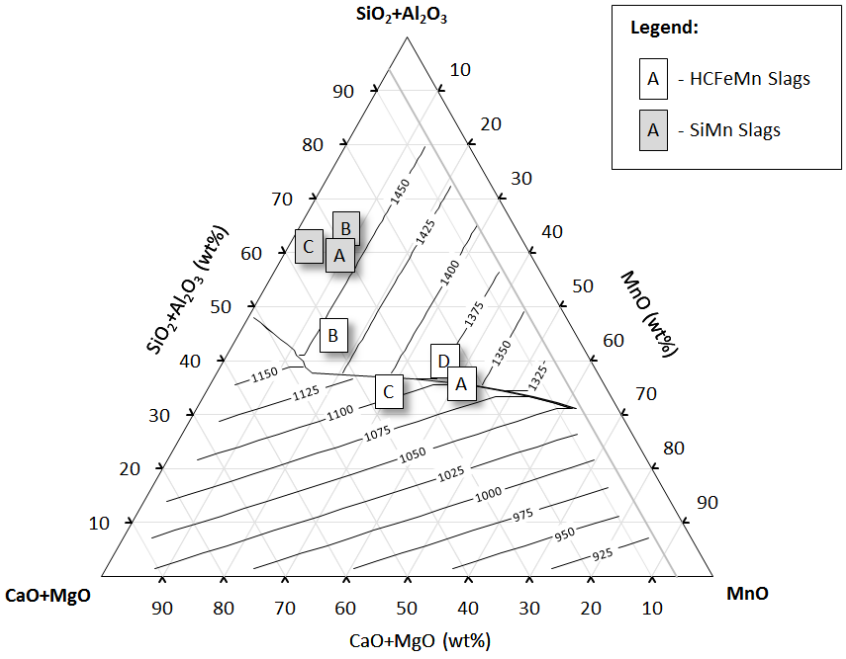

Fig. 10 Iso-heat capacity ternary diagram ($J.kg^{-1}.K^{-1}$) of the CaO-MnO-SiO_2-Al_2O_3-MgO slag system with 6% MgO and Al_2O_3/SiO_2=0.57 at 1500°C, showing SiMn and HCFeMn slag compositions (Table 1). Calculated using the models reported by Mills [5].

3.5.4 Conclusions

From the estimated heat capacity and enthalpy results, the following conclusions can be drawn:

- On average, solid slag heat capacities derived using the FactSage 6.2 [6] results are higher than those predicted with the models reported by Mills [5]. For liquid slags, however, heat capacities predicted with the models reported by Mills [5] are significantly higher than those by Björkvall [16] and FactSage 6.2 [6].
- Overall, for solid and liquid slags, heat capacities for SiMn slags are predicted higher than for HCFeMn slags, mostly due to the relatively high partial heat capacity of SiO_2 and its higher content in SiMn slags.
- As functions of basicity (Figure 9a), the enthalpies of SiMn slags are distinctively higher than those of HCFeMn slags due to the higher temperature of 1600°C compared with 1400°C for HCFeMn slags. The decrease of enthalpy with basicity is due to the basic oxides (CaO, MnO, MgO) having lower heat capacities than SiO_2 (and possibly Al_2O_3).

References

[1] F. Habashi, Handbook of Extractive Metallurgy, Wiley-VCH, Weinheim, 1997, 1, p 420–434.

[2] S.E. Olsen, M. Tangstad, T. Lindstad, Production of Manganese Ferroalloys, SINTEF and Tapir Academic Press, Trondheim, 2007.

[3] H.K. Versteeg, W. Malalasekera. An Introduction to Computational Fluid Dynamics – The Finite Volume Method,

2nd ed., Prentice Hall, Englewood Cliffs, New Jersey, 2007.

[4] Slag Atlas, 2nd ed., Verlag Stahleisen, Dusseldorf, 1995.

[5] K. C. Mills, L. Yuan, R.T. Jones. Estimating the physical properties of slags.*J. S. Afr. Inst. Min. Metall.*, 2011, 111, p 649–658.

[6] C.W. Bale, P. Chartrand, S.A. Degterov, G. Eriksson, K. Hack, R. Ben Mahfoud, J. Melançon, A.D. Pelton, S. Petersen. FactSage thermochemical software and databases, *CALPHAD: Comput. Coupling Phase Diagrams Thermochem.*, 2002, 26 (2), p 189–228.

[7] A. Kondratiev, E. Jak, P.C. Hayes. Predicting slag viscosities in metallurgical systems, *J. Met*, 2002, 54 (11), p 41–45.

[8] S. Seetharaman, K. Mukai, D. Sichen. Viscosities of slags – an overview. VII International Conference on Molten Slags, Fluxes and Salts, Johannesburg, Southern African Institute of Mining and Metallurgy, 2004, p 31–.

[9] K.C. Mills, B.J. Keene. Physical properties of BOS slags, *Int. Mater. Rev.*, 1987, 32, p 1-23.

[10] R.E. Aune, M. Hayashi, K. Nakajima, S. Seetharaman. Thermophysical properties of silicate slags. J. Met., 2002, 54 (11), 62–69.

[11] R. Roscoe. The viscosity of suspensions of rigid spheres. *Br. J. Appl. Phys.*, 1952, 3, p 267–269.

[12] K. Tang, M. Tangstad. Modelling Viscosities of Ferromanganese Slags, INFACON XI, New Delhi, India, Feb. 18-21 2007, Macmillan India, Delhi, 2007, p 344–357.

[13] J.D. Steenkamp, M. Tangstad, P.C. Pistorius. Thermal conductivity of solidified manganese-bearing slags – A preliminary investigation. Proceedings of Southern African Pyrometallurgy Conference, 6-9 March 2011, Cradle of Humankind, South Africa. R.T. Jones and P. den Hoed (eds). Johannesburg, Southern African Institute of Mining and Metallurgy, 2011, p 327–343.

[14] R. Eriksson, M. Hayashi, and S. Seetharam. Thermal diffusivity of liquid silicate melts. *Int. J. Thermophys.*, 2003, 24 (3), p 785–797.

[15] G. Zhang, K Chou. Model for evaluating density of molten slag with optical basicity, *J. Iron Steel Res. Int.*, 2010, 17 (4), p 1–4.

[16] J. Björkvall, Du Sichen, S. Seetharaman. Thermodynamic model calculations in multicomponent liquid silicate systems. *Ironmaking Steelmaking*, 2001, 28 (3), p 250–257.